Low rate of somatic mutations in a long-lived oak tree

Namrata Sarkar[1,2,3,†], Emanuel Schmid-Siegert[4,†], Christian Iseli[4,†], Sandra Calderon[4], Caroline Gouhier-Darimont[5], Jacqueline Chrast[1], Pietro Cattaneo[5], Frédéric Schütz[1], Laurent Farinelli[6], Marco Pagni[4], Michel Schneider[7], Jérémie Voumard[8], Michel Jaboyedoff[8], Christian Fankhauser[1*], Christian S. Hardtke[5*], Laurent Keller[2*], John R. Pannell[2*], Alexandre Reymond[1*], Marc Robinson-Rechavi[2,3*], Ioannis Xenarios[1,4,7*] and Philippe Reymond[5*]

[1]Center for Integrative Genomics, University of Lausanne, 1015 Lausanne, Switzerland, [2]Department of Ecology and Evolution, University of Lausanne, 1015 Lausanne, Switzerland [3]Evolutionary Bioinformatics Group, Swiss Institute of Bioinformatics, 1015 Lausanne, Switzerland, [4]Vital-IT Competence Center, Swiss Institute of Bioinformatics, 1015 Lausanne, Switzerland, [5]Department of Plant Molecular Biology, University of Lausanne, 1015 Lausanne, Switzerland, [6]Fasteris SA, 1228 Plan-les-Ouates, Switzerland, [7]Swiss-Prot group, Swiss Institute of Bioinformatics, 1211 Geneva, Switzerland, [8]Risk Analysis Group, Institute of Earth Sciences, University of Lausanne, 1015 Lausanne, Switzerland, [†]These authors contributed equally.

[*]Correspondence: christian.fankhauser@unil.ch, christian.hardtke@unil.ch, laurent.keller@unil.ch, john.pannell@unil.ch, alexandre.reymond@unil.ch, marc.robinson-rechavi@unil.ch, ioannis.xenarios@unil.ch, philippe.reymond@unil.ch

Because plants do not possess a proper germline, deleterious somatic mutations can be passed to gametes and a large number of cell divisions separating zygote from gamete formation in long-lived plants may lead to many mutations. We sequenced the genome of two terminal branches of a 234-year-old oak tree and found few fixed somatic single-nucleotide variants (SNVs), whose sequential appearance in the tree could be traced along nested sectors of younger branches. Our data suggest that stem cells of shoot meristems are robustly protected from accumulation of mutations in trees.

Accumulation of deleterious mutations is a fundamental parameter in plant ageing and evolution. Because the pedigree of cell division that generates somatic tissue is poorly understood, the number of cell divisions that separate zygote from gamete formation is difficult to estimate; this number is expected to be particularly large in trees and could in theory lead to a large number of DNA replication errors[1-3]. Tree architecture is determined by the modular growth of apical meristems, which contain stem cells. These cells divide and produce progenitor cells that undergo division, elongation and differentiation to form a vegetative shoot, the branch. Axillary meristems are formed at the base of leaf axils and are responsible for the emergence of side branches. They are separated from apical meristems by elongating internodes. In oak, early and repeated growth cessation of terminal apical meristems leads to a branching pattern originating from such axillary meristems. In turn, axillary meristems grow out and produce secondary axillary meristems. This process is reiterated indeterminately to produce highly ramified trees of large stature, resulting in thousands of terminal ramets[4]. The cumulative number of cell divisions separating meristems determines the rate of genetic aging and the potential accumulation of somatic mutations. To detect such mutations, we selected an iconic old oak tree (*Quercus robur*) known as the 'Napoleon Oak' by the academic community of the University of Lausanne. The tree was 22 years old when, on May 12, 1800, Napoleon Bonaparte and his troops crossed what is now

49   the Lausanne University campus, on their way to conquer Italy. At the time of sample harvest

50   for our study, the dividing apical meristems of this magnificent tree (Figure 1, Supplementary

51   Figure 1) had been exposed for 234 years to potential environmental mutagens, such as UV

52   and radioactive radiation.

53   To identify fixed somatic variants (i.e., those present in an entire sector of the

54   Napoleon Oak) and to reconstruct their origin and distribution among branches, we collected

55   26 leaf samples from different locations on the tree. We first sequenced the genome from

56   leaves sampled on terminal ramets of one lower and one upper branch of the tree. We then

57   used a combination of short-read Illumina and single-molecule real-time (SMRT, Pacific

58   Biosciences) sequencing to generate a *de novo* assembly of the oak genome. After removing

59   contigs <1000bp, we established a draft sequence of ca. 720 megabases (Mb) at a coverage of

60   ca. 70X, with 85,557 scaffolds and a N50 length of 17,014. Our sequence is thus in broad

61   agreement with the published estimated genome size of 740 Mbp[5]. The oak genome is

62   predicted to encode 49,444 predicted protein-coding loci (Supplementary Table 1).

63   We used two approaches to identify SNVs (single-nucleotide variants) between the

64   sequenced genomes of the two terminal branches. First, we aligned Illumina paired-reads on

65   the repeat-masked genome in combination with the GATK[6] variant caller. This allowed us to

66   establish a list of 3,488 potential SNV candidates with a high confidence score. From this list,

67   1,536 SNVs were experimentally tested by PCR-seq and only seven could be confirmed (see

68   Methods). Second, we used fetchGWI[7] to map read pairs to the non-masked genome. We

69   were able to call 5,330 potential SNVs from the mapped reads using a simple read pileup

70   process. Further analysis identified 82 putatively variable positions, including the seven

71   already identified using the repeat-masked genome analysis described above (see Methods).

72   Ten of the remaining 75 candidates from the second approach were confirmed by PCR-seq,

73   increasing the total number of confirmed SNVs separating the two genomes to 17 (Figure 1,

74   Supplementary Table 2), which were further confirmed by Sanger sequencing. Based on a
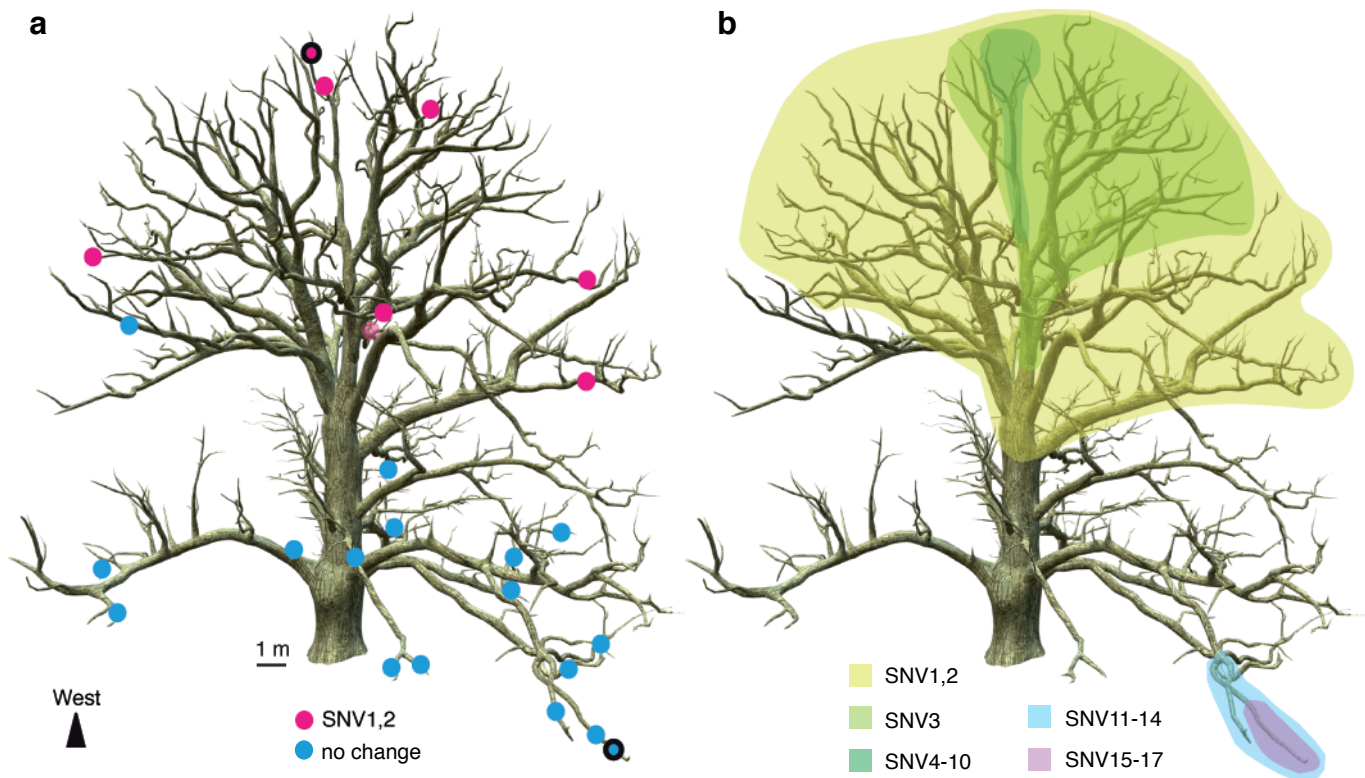
a

b

1 m

West

● SNV1,2
● no change

□ SNV1,2
□ SNV3
□ SNV4-10
□ SNV11-14
□ SNV15-17

Figure 1| Distribution of somatic mutations in the Napoleon oak. **a**, The genome of two leaf samples (outlined dots) was sequenced to identify single-nucleotide variants (SNV). 17 SNVs were confirmed and analysed in 26 other leaf samples to map their origin. A reconstructed image of the Napoleon Oak shows similar location of two SNVs (magenta dots) on the tree. Blue dots represent genotypes that are non-mutant for these SNVs. Three non-mutant samples are not visible on this projection. Location of other SNVs can be found in Supplementary Figure 2. **b**, Location of all identified SNVs. Sectors of the tree containing each group of SNVs are represented by different colours.

75 conservative estimate, we are likely to have missed no more than 18 further such sites (17

76 candidates and 1 false negative, see Supplementary Methods).

77 All 17 confirmed SNVs were heterozygous, as expected for novel somatic mutations.

78 Intriguingly, two SNVs were found on the same contig, separated by only 12 bp

79 (Supplementary Table 2). Sixteen SNVs occurred in introns or non-coding sequences that are

80 probably neutral. The remaining one (SNV1), which occurred in a large sector of the tree,

81 generates an arginine-to-glycine conversion in a putative E3-ubiquitin ligase (Supplementary

82 Table 2). The functional impact of exchanging a positively charged arginine with a non-

83 charged and smaller glycine residue is unknown and deserves further analysis.

84 Having confidently established 17 SNVs, we then assessed their occurrence

85 throughout the tree. We used Sanger sequencing to genotype the remaining 24 terminal

86 branches sampled from other parts of the tree and checked for the presence of each SNV.

87 SNVs were found in different sectors of the tree in a nested hierarchy that clearly indicates

88 the accumulation of mutations along branches during development (Figure 1, Supplementary

89 Figure 2). These results both provide independent confirmation of the originally identified

90 SNVs, and demonstrate their gradual, nested appearance and fixation in developmentally

91 connected branches during growth of the oak tree. Thus, while the exact ontogeny of the

92 Napoleon Oak may be difficult to reconstruct, our SNV analysis generated a nested set of

93 lineages supported by derived mutations, analogous to a phylogenetic tree.

94 The spontaneous mutation rate in plants has been estimated to range from 5×10^{-9} to

95 30×10^{-9} substitutions/site/generation, based on mutations accumulated during divergence

96 between monocots and dicots[8]. Values for mutation accumulation lines of *Arabidopsis*

97 *thaliana* maintained in the laboratory range between 7.0 and 7.4×10^{-9}, which corresponds to

98 ~1 mutation/genome/generation[9,10]. *Arabidopsis* is an annual plant that reaches

99 approximately 30 cm in height before producing seeds. In contrast, the physical distance

100 traced along branches between the terminal branches we sequenced for the Napoleon Oak is

101   about 40 m (Figure 1). Assuming similar cell sizes between oak and *Arabidopsis*, there

102   should have been about 133 times more mitotic divisions separating the extremes of somatic

103   lineages in Napoleon Oak than in *Arabidopsis* (4,000 cm/ 30 cm). Under the assumption that

104   the per-generation mutation rate is correlated with the number of mitotic divisions from

105   zygote to gametes of the next generation[1,11], and given the ~6-fold larger oak genome, we

106   thus initially estimated that the number of mutations/genome/generation rate should be ~800-

107   fold higher (133 X 6) for the Napoleon Oak than for Arabidopsis, i.e. ~800 SNVs/Napoleon

108   Oak genome. This value is much higher that the 17 SNVs we actually found, even under the

109   conservative assumption that we missed 18 other SNVs from the list of potential variants.

110   Our original hypothesis is thus not supported by the data and another mechanism has to be

111   invoked.

112   Classical studies of shoot apical meristem organization have reported that the most

113   distal zone has a significantly lower rate of cell division than more basal regions of the apex,

114   and might therefore be relatively protected from replication errors[12,13]. In a recent study that

115   followed the fate of dividing cells in the apical meristems of *Arabidopsis* and tomato, Burian

116   et al.[14] showed that an unexpectedly low number of divisions separate apical from axillary

117   meristems. In these herbaceous plants, axillary meristems are separated from apical meristem

118   stem cells by seven to nine cell divisions, with internode growth occurring through the

119   division of cells behind the meristem. The number of cell divisions between early embryonic

120   stem cells and terminal meristems thus depends more on the number of branching events than

121   on absolute plant size. Burian et al.[14] postulated that if the same growth pattern described

122   above for *Arabidopsis* and tomato applies to trees, their somatic mutation rate might be much

123   lower than is commonly thought, and the majority of fixed mutations should be found in

124   relatively small sectors as nested sets of mutations. Napoleon Oak's apical meristems are of

125   similar diameters to those of tomato[14] (Supplementary Figure 3) and show similar ontogeny.

126   It thus seems reasonable to suppose that the growth pattern described in *Arabidopsis* and

5

127   tomato is quite general in flowering plants and might also apply to long-lived trees. The low

128   number of SNVs and their nested appearance in sectors of the Napoelon Oak are thus

129   consistent with hypotheses proposed in Burian et al.[14].

130   Mutations accumulate with age, irrespective of plant stature, and long-term exposure

131   to UV radiation contributes to such changes. For the Napoleon Oak, the type of observed

132   SNVs were mostly G:C→A:T transitions, indicative of UV-induced mutagenesis (see

133   Supplementary Discussion). However, oaks protect their meristems in buds under multi-

134   layered leaf-like structures (Supplementary Figure 3), potentially reducing the incidence of

135   UV mutagenesis. The relatively low somatic mutation rate implied by our data may thus be

136   explained by the protective nature of oak bud morphology as well as by the pattern of cell

137   division predicted by Burian et al.[14]. Our results also suggest that mutations due to replication

138   errors in long-lived plants may be less important than environmentally induced mutations. In

139   this context, it is noteworthy that there was no evidence for an expansion of DNA-repair

140   genes in the oak genome compared to *Arabidopsis* (Supplementary Table 3).

141   To our knowledge, only two examples of functional mosaicism have been reported in

142   trees, a low incidence that might be attributable to the low somatic mutation rate that we

143   report. Although most non-neutral mutations should be maladaptive, eucalyptus trees have

144   been observed with a few branches that are biochemically distinct from the rest of the canopy

145   and have become resistant to Christmas beetle defoliation[15,16]. Functionally relevant somatic

146   mutations, such as SNV1 in our study, may thus occasionally contribute to adaptive evolution

147   if transferred to the fruits, but will more typically increase the genetic load of a population,

148   with implications for inbreeding depression and mating-system evolution (Supplementary

149   Discussion).

150   Our data give an unprecedented view on the limited role played by somatic mutations

151   in a long-lived organism, and support the view that stem cells in trees, although vulnerable to

152   environment-induced and replication-induced mutations, are probably quite well protected

153   from them. Consistent with this finding, a recent study in *Arabidopsis* has shown that the

154   number of cell divisions from germination to gametogenesis is independent of life span and

155   vegetative growth[17]. Future studies on different tree species and older specimens are needed

156   to test the generality of our study. This work also illustrates the potential for analyses of

157   multiple genomes from single individuals, which throw exciting new light on the rate,

158   distribution and potential impact of somatic mutations in both plant and animal tissues[18,19].

159

160   **Methods**

161   **Materials and genome sequencing**. Leaves were collected in April 2012 from the terminal

162   part of a lower (sample 0) and an upper branch (sample 66) of the Napoleon Oak (*Q. robur*)

163   on the Lausanne University Campus (Switzerland, 46°31'18.9"N 6°34'44.5"E). The age of the

164   tree was estimated by a tree ring analysis from a sample taken at the basis of the trunk

165   (Laboratoire Romand de Dendrochronologie, 1510 Moudon, Switzerland). DNA from the

166   two samples was extracted and the genome sequenced. Paired-end sequencing libraries with

167   insert size of 400 bp were constructed for each DNA sample according to the manufacturer's

168   instructions. Then, 100 bp paired-reads were generated on Illumina HiSEq 2000 at Fasteris

169   (www.fasteris.com). In addition, 3 kb mate-pair libraries from sample 0 were constructed and

170   sequenced with single-molecule real-time (SMRT) technology according to the

171   manufacturer's instructions (Pacific Biosciences). Short reads were combined with PacBio

172   reads to assemble a reference genome (Supplementary Methods).

173

174   **SNV identification**. We used two different methods to identify SNVs (see flowchart,

175   Supplementary Figure 4). In the first one, Illumina reads (278,547,120 and 278,651,792 for

176   sample 0 and 66, respectively) were aligned to the masked (RepeatMasker, v4.05) *de novo*

177   assembly   with   Bowtie2   (v2.2.2,   https://sourceforge.net/projects/bowtie-

178   bio/files/bowtie2/2.2.2) using default parameters. GATK[6] v2.5.2 was used for local

179   realignment and variant calling using standard hard filtering parameters according to GATK

180   Best Practices recommendations[20]. Prior to variant calling, each sample was screened for

181   duplicates using PICARD tools (http://broadinstitute.github.io/picard/ v2.9.0,

182   MarkDuplicates). Variants with confidence score $\geq$50 were retained further. We identified

183   1,832,554 heterozygous sites common to both samples, as well as 314,865 putative

184   differences between sample 0 and 66 (165,489 sites predicted to be homozygous on sample 0

185   and heterozygous on sample 66 and 149,376 homozygous on sample 66 and heterozygous on

186   sample 0). The distribution of the confidence scores of the 1,832,554 heterozygous sites

187   common to both samples was a superposition of a Gaussian distribution, peaking at 910,

188   possibly representing true positives, and of an exponential distribution, possibly representing

189   the decreasing number of false positives with regard to increasing confidence score.

190   Importantly, the distribution of scores of the sites with putative differences between samples

191   was an exponential distribution of very low values, similar to the potential false positives of

192   shared heterozygote sites. We thus hypothesized that sites that are truly different between

193   samples 0 and 66 were unlikely to be present at sites with a confidence score below 300.

194   From 3,488 putative SNVs with a confidence score $\geq$300 on the heterozygous sites and $\geq$200

195   on homozygous sites, we selected 1,536 SNVs for validation by PCR-seq (Supplementary

196   Methods). We identified only 7 true SNVs that were further confirmed by Sanger sequencing.

197   This low rate is consistent with the expectation from the distribution of GATK scores for

198   these sites.

199   In the second method, Illumina reads of samples 0 and 66 were mapped against the

200   non-masked oak genome assembly. The genome was 719,779,348 bp long, but 69,130,634

201   (9.52%) of those nucleotides were gaps and were discarded, leaving an actual search space of

202   650,648,714 bp. Of the latter, 458,143,725 nucleotides with a read coverage $\geq$8 in both

203   samples were analysed further. The mapping process was performed at the read pair level by

204   the genome mapping tool, fetchGWI[7], followed by a detailed sequence alignment tool,

205   align0[21]. Potential SNVs were called from the mapped reads by a simple read pileup process

206   followed by detection of positions where the pileup shows variations with respect to the

207   reference genome; this produced a list of 5,330 positions. Those positions were browsed

208   through a local adaptation of the samtools pileup browser[22] to evaluate the quality of the

209   mapping in the surrounding region and to discriminate between well-assembled high-quality

210   regions with two alleles per sample, or low complexity and possibly badly assembled

211   repeated regions. Criteria for selection were ≥8 reads in each orientation (see above); 100%

212   homozygosity site for one sample and at least 30% minor allele frequency for the other

213   sample with variants in both orientations; and coherent sequence ±50 bp from variant site.

214   This manual process led to the selection of 82 putative variable positions, including the seven

215   already identified. Upon experimental validation, 10 of the remaining 75 candidates were

216   confirmed by PCR-seq and Sanger sequencing. The Food and Drug Administration (FDA)

217   has evaluated this approach in an effort to assess, compare, and improve techniques used in

218   DNA   testing   on   human   genome   variation   analysis

219   (https://precision.fda.gov/challenges/consistency). Within this frame, our method reached a

220   F-score (F-score evaluates precision and recall) over 95% comparable to other identifiers like

221   BWA coupled with GATK.

222

223   **SNV Genotyping**. Leaf DNA from different locations on the tree was prepared and amplified

224   using primers located 100-150 bp away from the 17 confirmed SNVs (Supplementary Table

225   4). Amplicons were then subjected to Sanger sequencing.

226

227   **Data availability.** All Illumina reads and SMRT sequences have been deposited in GenBank

228   under accession BioProject PRJNA327502.

229

230

9

References

1. Scofield, D.G. & Schultz, S.T. Mitosis, stature and evolution of plant mating systems: low-Φ and high-Φ plants. *Proc. Royal Soc. London B: Biol. Sci.* **273**, 275–282 (2006).

2. Ally., D., Ritland, K. & Otto, S.P. Aging in a long-lived clonal tree. *PLoS Biol.* **8**, e1000454 (2010).

3. Bobiwash, K., Schultz, S.T. & Schoen, D.J. Somatic deleterious mutation rate in a woody plant: estimation from phenotypic data. *Heredity* **111**, 338–344 (2013).

4. Millet, J. L'architecture des arbres des régions tempérées: son histoire, ses concepts, ses usages. *MultiMondes ed.*, 397 pp (2012).

5. Plomion, C. *et al.* Decoding the oak genome: public release of sequence data, assembly, annotation and publication strategies. *Mol. Ecol. Resour.* **16**, 254-265 (2016).

6. McKenna, A. *et al.* The genome analysis toolkit: a MapReduce framework for analyzing next-generation DNA sequencing data. *Genome Res.* **20**, 1297-303 (2010).

7. Iseli, C., Ambrosini, G., Bucher, P. & Jongeneel, C.V. Indexing strategies for rapid searches of short words in genome sequences. *PLoS One* **2**, e579 (2007).

8. Wolfe, K.H., Li, W.H. & Sharp, P.M. Rates of nucleotide substitution vary greatly among plant mitochondrial, chloroplast, and nuclear DNAs. *Proc. Natl. Acad. Sci. USA* **84**, 9054–9058 (1987).

9. Ossowski, S. *et al.* The rate and molecular spectrum of spontaneous mutations in *Arabidopsis thaliana*. *Science* **327**, 92–94 (2010).

10. Yang, S. *et al.* Parent–progeny sequencing indicates higher mutation rates in heterozygotes. *Nature* **523**, 463-467 (2015).

11. Scofield, D.G. Medial pith cells per meter in twigs as a proxy for mitotic growth rate (Φ/m) in the apical meristem. *Am. J. Bot.* **93**, 1740-1747 (2006).

12. Romberger, J.A., Hejnowicz, Z. & Hill, J.F. Plant structure: function and development. *Springer-Verlag ed.*, 524 pp (1993).

13. Kwiatkowska, D. Flowering and apical meristem growth dynamics. *J. Exp. Bot.* **59**, 187-201 (2008).

14. Burian, A., Barbier de Reuille, P. & Kuhlemeier, C. Patterns of stem cell divisions contribute to plant longevity. *Curr. Biol.* **26**, 1385-1394 (2016).

15. Edwards, P.B., Wanjura, W.J., Brown, W.V. & Dearn, J.M. Mosaic resistance in plants. *Nature* **347**, 434 (1990).

16. Padovan, A., Lanfear, R., Keszei, A., Foley, W.J. & Külheim, C. Differences in gene expression within a striking phenotypic mosaic *Eucalyptus* tree that varies in susceptibility to herbivory. *BMC Plant Biol.* **13**, 29 (2013).

17. Watson, J.M. *et al.* Germline replications and somatic mutation accumulation are independent of vegetative life span in *Arabidopsis*. *Proc. Natl. Acad. Sci.* USA **113**, 12226–12231 (2016).

18. Behjati, S. *et al.* Genome sequencing of normal cells reveals developmental lineages and mutational processes. *Nature* **513**, 422–425 (2014).

19. Lodato, M.A. *et al.* Somatic mutation in single human neurons tracks developmental and transcriptional history. *Science* **350**, 94–98 (2015).

20. Van der Auwera, G.A. *et al.* From FastQ data to high-confidence variant calls: the genome analysis toolkit best practices pipeline. *Curr. Protocols Bioinfo.* **43**, 11.10.1-11.10.33 (2013).

21. Myers, E.W. & Miller, W. Optimal alignments in linear space. *Comput. Appl. Biosci.* **4**, 11-17 (1988).

22. Li, H. *et al.* The Sequence alignment/map (SAM) format and SAMtools. *Bioinformatics* **25**, 2078-9 (2009).

281

293

Author contributions

L. F. sequenced the genome. E.S.-S., S.C., M.P. assembled and annotated the genome. N.S., E.S.-S., C.I. identified SNVs. C.G.-D., J.C. extracted DNA and confirmed SNVs. E.S.-S., M.R.-R. analyzed genome duplication. P.C. produced cross-sections of oak apical meristems. M. S. established a list of DNA repair genes. F. S. provided statistical help with the analyses. J.V., M.J. produced a 3D model of the oak tree. C.H., C.F., L.K., I.X., M.R.-R., J.P., A.R., P.R. conceived the project and wrote the manuscript.
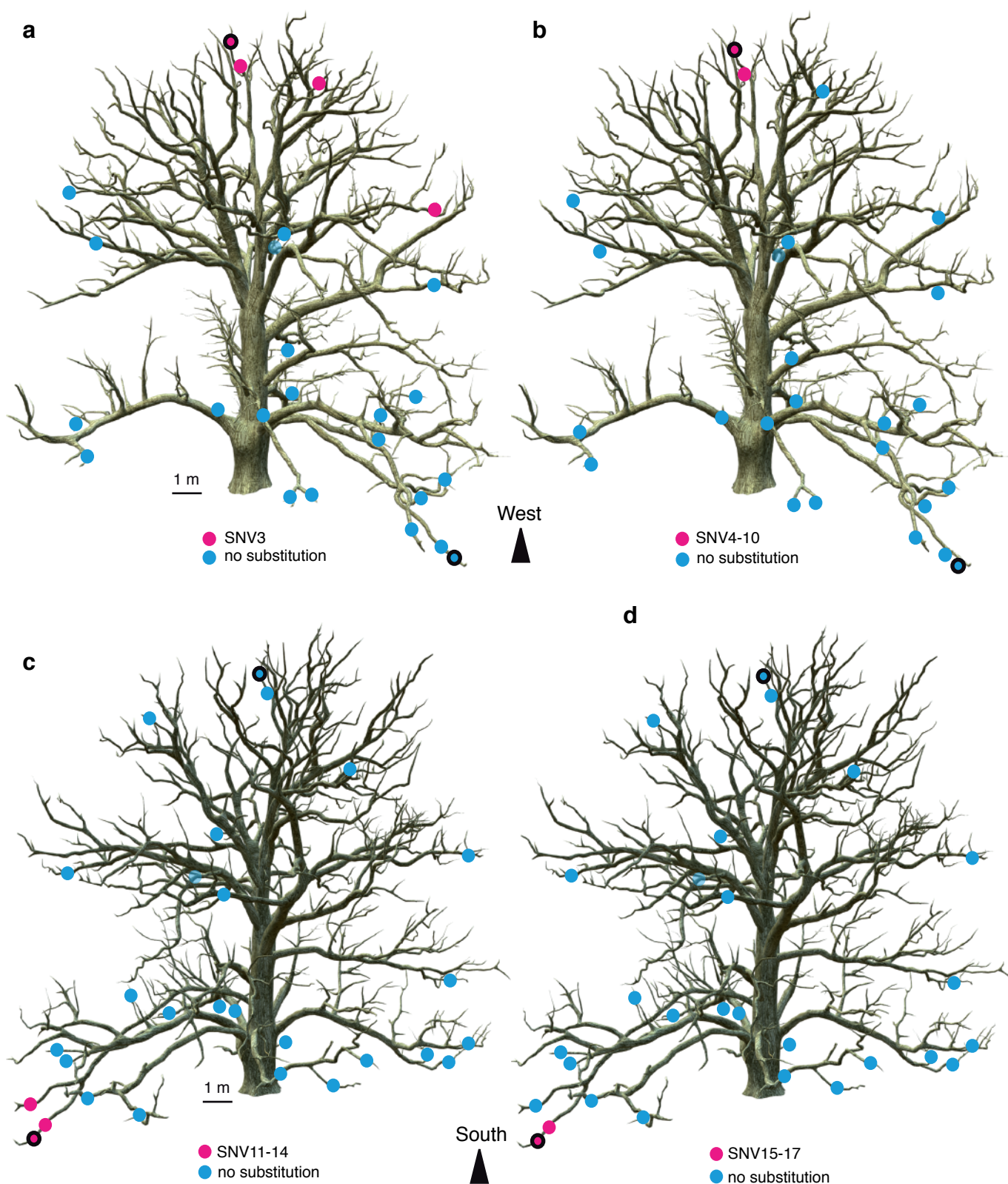
301

Additional information

Supplementary information is available for this paper.

Correspondence and requests for materials should be addressed to P. R.

11
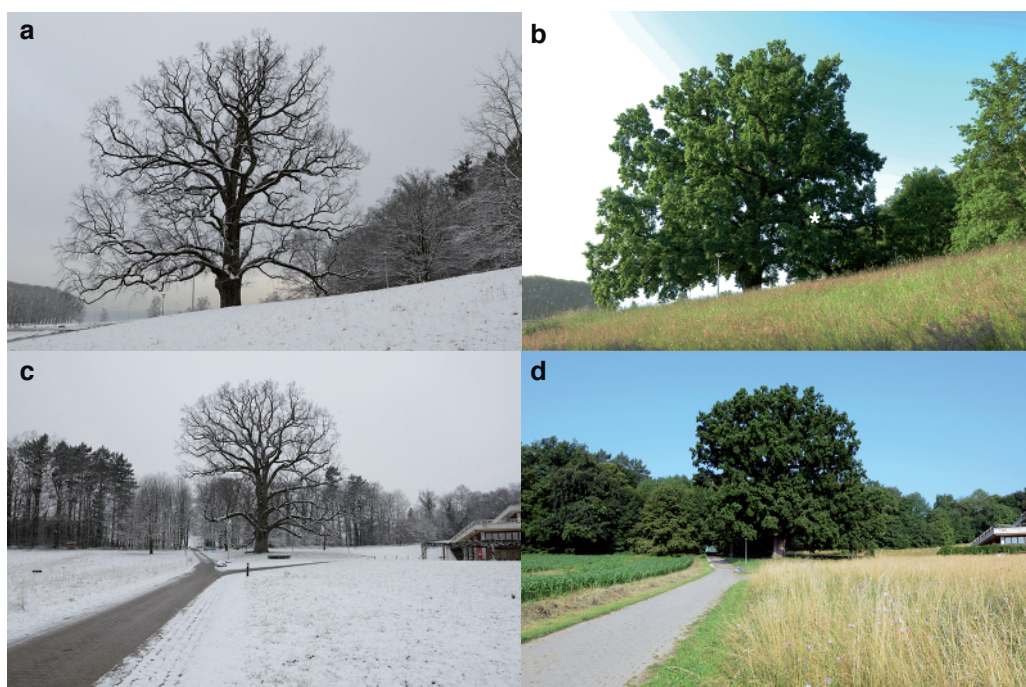
Supplementary Figure 1 | Napoleon Oak. Photographs of the Napoleon Oak on the Lausanne University campus taken in winter and summer. **a, b,** South view. **c, d,** North-West view.

Supplementary Figure 2 | Distribution of somatic mutations in the Napoleon Oak. The genome of two leaf samples (outlined dots) was sequenced to identify single-nucleotide variants (SNV). 17 SNVs were confirmed and analysed in 26 other leaf samples to map their origin. **a-d,** Reconstructed images of the Napoleon Oak show the location of different SNVs (magenta dots) on the tree. Blue dots represent genotypes that are non-mutant for these SNVs.
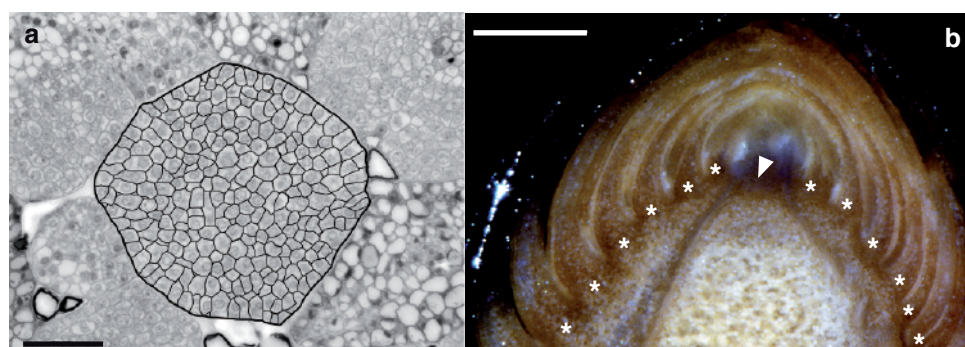
Supplementary Figure 3 | Napoleon Oak apical meristem. a, Cross-section of an apical meristem. Meristematic cells are delineated. Surrounding cells belong to leaf-like structures surrounding the meristem. Scale bar, 50 mm. **b**, Longitudinal section of an apical bud. Apical meristem (arrowhead) is surrounded by leaf-like structures (stars). Scale bar, 500 mm.
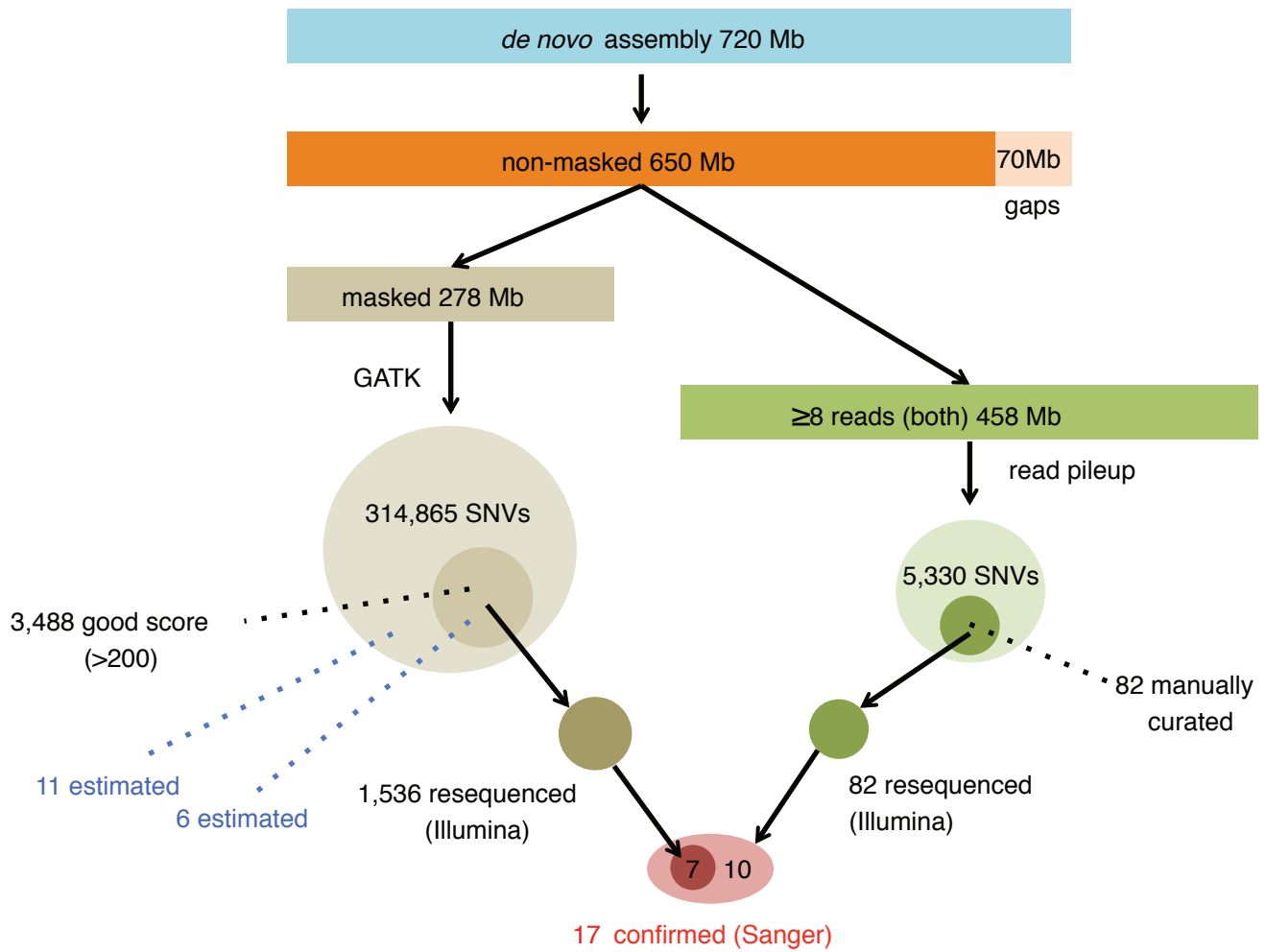
Supplementary Figure 4 | Flowchart of SNV identification methods.
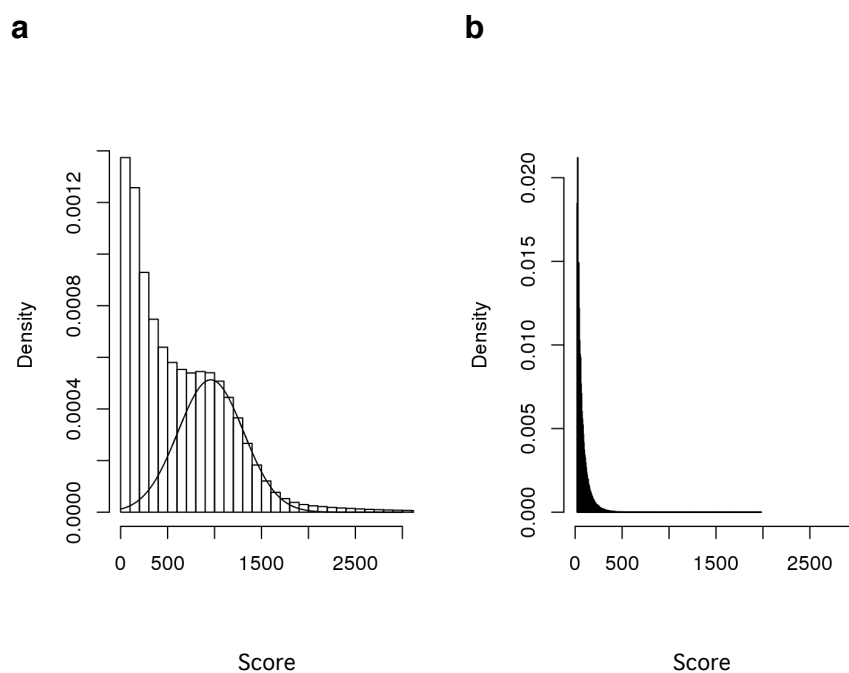
Supplementary Figure 5 | Distribution of variants. a, Distribution of the confidence scores of the 1'832'554 heterozygous sites common to both samples 0 and 66. **b,** Distribution of the confidence scores of 165'489 heterozygous sites in sample 66 that are homozygous in sample 0.
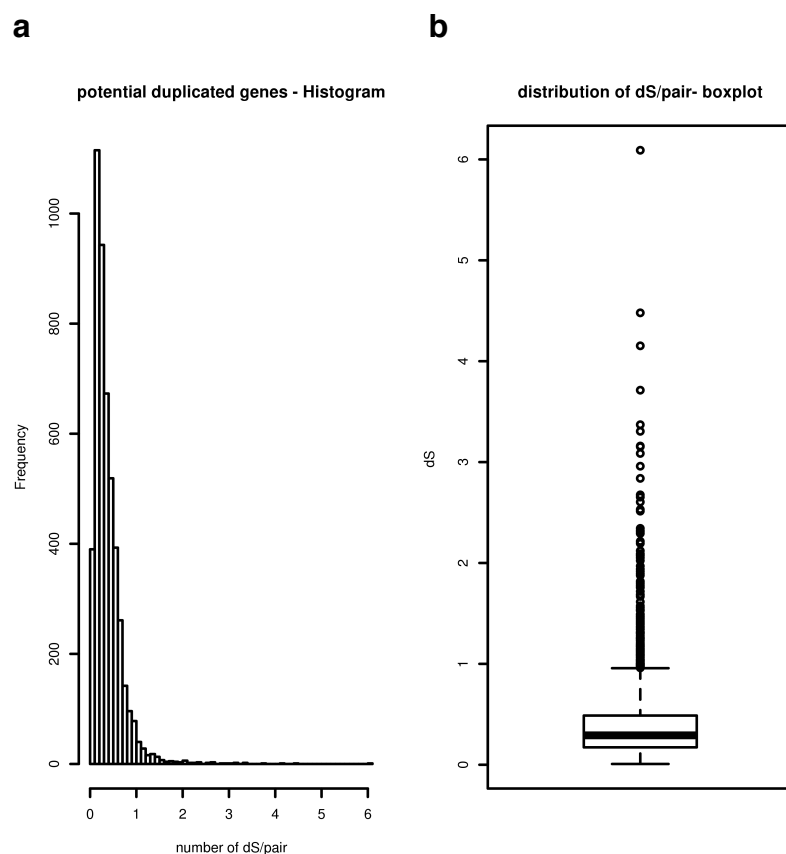
Supplementary Figure 6 | Analysis of oak genome duplication. a, Frequency plot and **b**, box plot showing the distribution of synonymous distances (dS) on a stringent set of 4,777 paralog pairs. This analysis was done with a threshold BLAST E-value <1e-10 and by removing multigene families of more than 20 members.
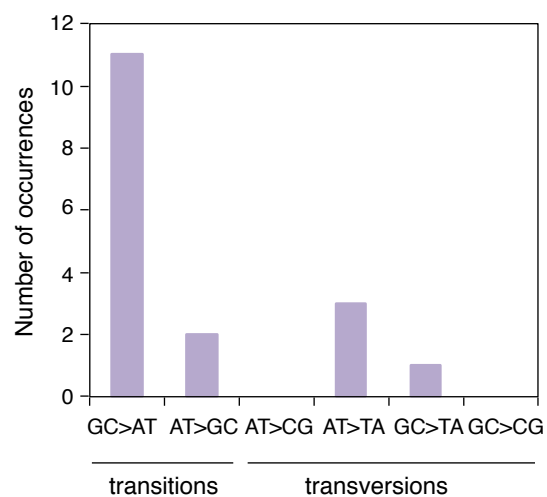
Supplementary Figure 7 | Spectrum of somatic mutations between two Napoleon Oak genomes.
The type of substitution for 17 confirmed oak SNVs is shown.

Supplementary Table 1: *Quercus robur* genome statistics.

Genome	
Total genome length (bp)	719,779,348
Number of scaffolds	85,557
Maximum scaffold length (bp)	317,245
NG50 based on 740 Mbp (bp)	17,014
Gaps (%)	9.52
Masked (%)	39.84
Genes	
Average length (bp)	2,360
Maximum length (bp)	47,221
Average intron length (bp)	740
Average exon length (bp)	232
Proteome	
Total predicted proteins	49,444
Full proteins	44,096
Partial proteins	5,348
Nb proteins with orthologous in *Glycine max*	39,656
Nb orthologous in *Glycine max* + functional annotation	16,323
Nb orthologous in *Glycine max* + function via ATH	23,333

Supplementary Table 2. SNVs in the Napoleon Oak.

SNV	Contig	Lower branch genome (0)	Upper branch genome (66)	Context	Position
SNV1	Contig12293_20040	TCTGA	TCT/CGA		Exon (R→G)
SNV2	Contig8610_5366	AACAG	AAC/TAG	CpNG	Intron
SNV3	Contig17717_5512	ACCAT	ACC/TAT	dipyrimidine	Non coding
SNV4	Contig19224_2528	TACAT	TAC/TAT		Non coding
SNV5	Contig3344_66711	AACGC	AAC/TGC	CpG	Non coding
SNV6	Contig420_15205	CTTGA	CTT/AGA		Non coding
SNV7	Contig46021_5283	TCCTA	TCC/TTA	dipyrimidine	Non coding
SNV8	Contig4756_544	AAGGT	AAG/AGT	dipyrimidine	Intron
SNV9	Contig61424_5311	ATTTG	ATT/ATG		Non coding
SNV10	Contig79811_6871	AACAA	AAC/TAA		Non coding
SNV11,12	Contig33320_1101-13	ACC/ATTTACGAGGCTA/TTT	ACCTTTACGAGGCTATT		Non coding
SNV13	Contig1217_8596	TCG/AGG	TCGGG	dipyrimidine	Non coding
SNV14	Contig15467_11236	AGG/AAT	AGGAT	dipyrimidine	Intron
SNV15	Contig4515_9475	GTC/TGT	GTCGT	CpG, dipyrimidine	Intron
SNV16	Contig28929_3009	TTT/CGG	TTTGG		Non coding
SNV17	Contig32076_9167	TGG/AGC	TGGGC	dipyrimidine	Non coding

Mutated bases are shown in red. Homozygous sites generate heterozygote sites.

Supplementary Table 3. Orthology and duplication of DNA repair genes in oak and peach trees.

Branch of the phylogeny	DNA repair genes			All genes		
	duplicated	total	% total	duplicated	total	% total
Quercus robur	0	228	0.0	258	10,199	3.5
Prunus persica	5	228	2.2	860	16,004	5.4
Quercus - Prunus common ancestor	1	228	0.4	523	8,474	6.2

All gene counts are for *Arabidopsis thaliana* orthologs; the number of "all genes" varies according to the number of orthologs detected for each set (i.e., from *Quercus robur*, from *Prunus persica*, or shared). All orthology detection and lineage-specific duplication calls are from OMA (see Experimental Procedures)

Supplementary Table 4. List of primers used for genotyping and Sanger sequencing

SNV	Contig	Forward primer (5'-3')	Reverse primer (5'-3')
SNV1	Contig12293_20040	CCCTTGCCTGTAAGGAATCA	TGCTATGCTTGGAAAAACCA
SNV2	Contig8610_5366	GGCTGAACAAAGTTGAGTGGA	TGTAAGCCCTCATCCCATGT
SNV3	Contig17717_5512	CAACGAACTCACAGGACGTG	AGCTTTGTCATCAGCCTTCAG
SNV4	Contig19224_2528	CTTTTTACAATGCCCCCAGA	AAATGCAAGACATCGCTCCT
SNV5	Contig3344_66711	AGAAAATGTGGACGCTGACC	GCCGTATTGTTGTTGGGAAC
SNV6	Contig420_15205	CGAGCATTGATCGAATACCA	TGTGGCCATCCAAGATTAAA
SNV7	Contig46021_5283	AACTGTCGAGCATTGGGTTT	GGATTGCCAAAAGGAGGAAT
SNV8	Contig4756_544	GGCAGGCAGAGACACAAACT	GGAGAGTGGTGGGAATTTGA
SNV9	Contig61424_5311	GCATCGACCAACTGGTTTTT	CAGTTGCCCTCCATTTGATT
SNV10	Contig79811_6871	CCCAAAAAGTTCCAGCTCAG	ATGACGACTAAGGGCGTGTT
SNV11	Contig33320_1101	GATTGGATGTGGGATCCTTG	GGCAATTTCACTACCCTTGG
SNV12	Contig33320_1113	GATTGGATGTGGGATCCTTG	GGCAATTTCACTACCCTTGG
SNV13	Contig1217_8596	CGACAGATGCTGCTATCGAG	AACGATGAAGATCAGGAAGCA
SNV14	Contig15467_11236	TCTGTGATCCACGTGTTGGT	GGCGCCTAAACAAGTCTCAG
SNV15	Contig4515_9475	TTGGCCTATATTTGAAACCAAT	AGTCGGCAAATCCAAAATTC
SNV16	Contig28929_3009	AGCACCCGATAAGCTCAAAA	GTCTTCAGCTCTGCCACCTC
SNV17	Contig32076_9167	TTCATTGCAATTTCCACAGG	TCATCATCCAAGCCTGACG

1   **Low rate of somatic mutations in a long-lived oak tree**

2   Sarkar *et al.*

3

4   **<u>Supplementary Methods</u>**

5   **Genome assembly**. For sample 0, a paired-end library generated 2 x 151,194,704 reads

6   (coverage 40X) and a mate-pair library generated 2 x 107,264,298 reads (coverage 29X). For

7   sample 66, a paired-end library generated 2 x 158,505,474 reads (coverage 42X) and a mate-

8   pair library generated 2 x 124,076,608 reads (coverage 33X). These reads were filtered and

9   trimmed prior assembly using Trimmomatic (v0.3; leading:3, trailing:3, slidingwindow:4:15,

10   minlen:36, custom adapter library)[23] and assembled using SOAPdenovo2 (v2.04.240, kmer

11   49)[24]. In a second step the assembly was scaffolded with mate-pairs using the same program.

12   The assembly was further scaffolded with long single-molecule PacBio reads (22 SMRT

13   cells, XL-C2 and P4-C2 chemistry, coverage 19X) and the program AHA

14   (http://www.pacb.com/products-and-services/analytical-software/smrt-analysis/; SMRTPipe

15   2.0.1 manually driven, settings (5,2,50,70), no gap-filling). Assembled sequences <1000 bp

16   were removed to facilitate further analysis. The genome was extended with all paired-end

17   libraries and SSPACE[25] (v2.0, -x = 1,z = 0,-k = 5,-a = 0.7,-n = 15,-T = 20,-p = 0,-o = 20,-t =

18   0,-m = 32,-r = 0.9) and gaps were filled using Gapfiller (v1.10, all paired-end libraries)[26].

19   We screened the paired-end libraries for potential non-oak sequences using metaphlan

20   (v1.7.7)[27]. Based on metaphlan results, reference genomes were obtained for the non-oak

21   genomes and the oak scaffolds were filtered against these using blast (ncbi-blast v2.28, >90%

22   sequence identity and E-value <1e-5). The genome was next scaffolded again using the

23   PacBio reads and PBJelly (v14.1.14)[28]. If not further specified, programs were used with their

24   standard settings.

25

26   **Gene prediction and annotation**. Repetitive elements were analysed by first generating a

27   specific repeat model using RepeatModeler (http:/www.repeatmasker.org; v1.0.7, -engine

28   wublast). Repetitive regions in the genome were subsequently masked with the obtained

29   model using RepeatMasker (http:/www.repeatmasker.org; v4.0.3). Genes were predicted by

30   generating a *Q. robur* specific gene prediction model for Augustus (v3.0.1)[29], as described in

31   Tran et al.[30]. Instead of RNAseq reads, we used the UniProtKB reference proteome of

32   *Glycine max* mapped with the splice aware mapper exonerate   (V2.2.0, model

33   protein2genome, geneseed 250 –minintron 20, --maxintron 20000)[31]. Using this model we

34   predicted genes and subsequently their encoded proteins for the hard-masked version of the

35   genome (settings: no hints, no UTR predicted, no alternative transcripts). Non-coding

36   elements were annotated using RFAM (v1.5; infernal 1.0.2; blast 2.2.26; hmmer 3.1b1)[32] in

37   the genome with coding regions masked but repetitive elements unmasked. The predicted

38   proteome   was   annotated   based   on   homology   using   the   FASTA   toolkit

39   (http://www.ebi.ac.uk/Tools/sss/fasta/; v36.3.5e) as following: proteins from the *Glycine max*

40   proteome were first mapped with ggsearch (-b 1 -d 0 -E 1e-5 -m 8 -T 10); proteins that did

41   not map were mapped in a next step with glsearch (-b 1 -d 0 -E 1e-5 -m 8 -T 10) and finally

42   the rest with ssearch (-b 1 -d 0 -E 1e-5 -m 8 -T 10). The functional protein annotation was

43   overtaken from *Glycine max*. For proteins with unknown function in *Glycine max,* we

44   extended the annotation using the OMA database (www.omabrowser.org) and orthologous

45   proteins from *Arabidopsis*. PFAM[33] was used additionally to obtain functional domain

46   annotations for the proteome and the concatenated proteome annotation was transferred onto

47   the oak genome.

48

49   **PCR-seq.** A modification of the published RT-PCR-seq method[34] was used. Briefly, pairs of

50   primers for 50-150 bp amplicons containing the targeted sequence were designed using

51   Primer3. Touchdown PCR amplification was performed in a final volume of 12.5 ml with

2

52   JumpStart REDTaq ReadyMix (Sigma-Aldrich), a primer concentration of 0.4 mM and 2 ng

53   of gDNA per reaction in 384-well plates. Equal volumes of PCR products were pooled for

54   each DNA template (sample 0 and 66). One ml of each pool was then purified with the

55   QIAquick PCR Purification Kit (Qiagen) following the manufacturer's instructions. The

56   KAPA LTP Library Preparation Kit (Kapa Biosystems) was used, starting with 500 ng of

57   purified PCR products, to create a library compatible with an Illumina sequencing platform.

58   Clean-ups between enzymatic steps were performed with Nucleospin PCR Clean-up columns

59   (Macherey-Nagel). After ligation of pentabase adapters, libraries were run on a 2 % agarose

60   gel and extracted using the MinElute Gel Extraction kit (Qiagen). Libraries were sequenced

61   on HiSeq 2000 after six cycles of amplification (Lausanne Genomic Technologies Facility).

62   Amplicon reads were aligned, with no mismatches allowed, to a compendium of the expected

63   amplimers that bore the reference allele, the alternate allele identified in the heterozygote

64   sample, as well as the remaining two nucleotides at the variable position; this allowed an

65   unbiased estimation of the error rate generated by the sequencing itself. As this method might

66   have missed *bona fide* changes between the two sampled branches that present other

67   heterozygous sites close by, we also aligned amplicon sequencing reads directly to the

68   reference genome, with mismatches allowed.

69

70   **Estimation of the possible missed SNVs.** About half of the putative variable sites with

71   confidence scores ≥200 were assessed experimentally by PCR-seq (1,536 out of 3,488 sites).

72   Given the confidence scores of the tested sites, we estimated that we missed fewer than 6

73   SNVs in the sites not evaluated by PCR-seq. We then evaluated the number of true positives

74   missed within candidates with confidence scores <200 in the list of sites that were

75   heterozygous in only one sample. We fitted a mixture of two distributions, including a

76   normal distribution that should fit the correct calls, modelled on the 1,832,554 sites that were

77   predicted to be heterozygous in both samples (Supplementary Figure 5a). Applying this

78 distribution to the data for sites that are homozygous on sample 0 and heterozygous on

79 sample 66 (case 1, Supplementary Figure 5b), we find that the distribution of correct calls is

80 insignificant compared to the rest. In details, when fitting this normal distribution to the data,

81 the expected number of correct calls with a score < 200 is 5.24. Extrapolating this calculation

82 for sites that are heterozygous on sample 0 and homozygous on sample 66 (case 2), we

83 estimate that we have missed fewer than 11 true SNVs for both cases. We thus estimate a

84 total of 17 missed SNVs (6 with a score ≥200 and 11 with a score <200). Note that we did not

85 assess the presence of larger somatic changes such as copy number variants, small indels, and

86 transposition events.

87

88 **Estimation of the false negative rate.** A few recent studies have tried to estimate the false

89 negative rate of SNV calling for large genomes assembled with short read sequences[10,35]. The

90 main method used in those studies was to introduce simulated SNVs into the data, and check

91 how well they were recovered. This is not directly applicable to our approach, as we did not

92 merely perform bioinformatics filtering, but also used a large PCR-seq screen to detect

93 SNVs. The comparison of F2 / F4 genotypes is very promising, but cannot either be applied

94 to our data[10]. It is notable that both approaches, in Drosophila[35] and in Arabidopsis[10], found

95 very low rates of false negatives, less than 2%. If this holds true for our data (which has

96 higher mean read coverage), then our false negative rate cannot be so large as to challenge

97 our main conclusions. Using this maximum rate of 2%, we can estimate the number of false

98 negatives (FN) as: $0.02 = FN/FN + TP$, where TP equals 34 estimated true SNVs. This

99 calculation gives 0.69, which suggests that we have only missed ~1 SNV.

100

101 **Whole-genome duplication**. Simple clustering based on homology, (i.e., clustering the

102 predicted proteins by identity, CD-HIT, min 90% similarity), retrieved 1,098 proteins that

103 have a >90% identity to another protein, which is not suggestive of recent whole genome

104   duplication. Whole genome duplication should lead to an excess of relatively old paralogs,

105   whereas small-scale duplicates are expected to be enriched in very recent paralogs. This can

106   be estimated from the distribution of synonymous distances (dS)[36,37]. We computed the dS on

107   a stringent set of 4,777 paralog pairs with BLAST E-value <1e-10, removing large multigene

108   families (more than 20 members). The distribution of dS values is clearly unimodal, with an

109   excess of low dS values (i.e., young paralogs, Supplementary Figure 6). This also does not

110   support a recent whole genome duplication in the oak lineage.

111   To address the possibility of a more ancient duplication event, we compared our oak

112   genome reference with itself using "BLAST all versus all" as suggested in Panchy et al.[38],

113   (i.e., similarity ≥30%, match length ≥150AA and E-value ≤1e-5). Following this procedure

114   we have 49,444 proteins, of which 3,650 are duplicated (7.4%), 2,070 are triplicated (4.1%)

115   and 23.7% are present in more copies with diminishing frequency. In summary, a total of

116   17,474 oak proteins out of 49,444 appear to be duplicated (35%), which is less than that

117   reported for closely related species (e.g. *Medicago sativa* has about 50,000 genes of which

118   >75% are duplicated, according to Panchy et al.[38]). We then assessed whether the similarity

119   identified above was local, properties of similar domains, or extended along the entire

120   protein, indicative of duplicated proteins. We found only 973 oak proteins that have

121   duplications extending over their entire lengths. In summary, it is possible that the oak

122   genome underwent duplication, as suggested by Panchy et al.[38], but this event appears to be

123   rather old, as we have very few (<3%) duplicated genes with very high similarity (>90%) and

124   no second peak in the dS distribution (Supplementary Figure 6). It seems unlikely that such a

125   duplication event should compromise the identification of *bona fide* variants. Note that if the

126   duplication would have hindered the capacity to detect these variants, they would not be

127   found in nested sectors of the tree but rather in all 26 samples assessed.

128

129   **Analysis of DNA repair genes**. Orthologs between *Arabidopsis*, *Prunus persica* (peach) and

130   *Q. robur* were called using the OMA database[39]. One-to-many orthologs, e.g., between

131   *Arabidopsis* and *Q. robur*, represent duplication in the oak lineage since the divergence from

132   *Arabidopsis*; they are also known as in-paralogs of oak. We classified these in-paralogs

133   according to whether the duplication was shared by *P. persica* and *Q. robur* (i.e., one copy in

134   *Arabidopsis* relative to several copies in both the peach and oak genomes), or whether it was

135   peach- or oak-specific (i.e., one copy in *Arabidopsis* and peach, relative to several copies in

136   oak). The number of duplicates was reported as the number of genes that could be called

137   duplicate (i.e., the number of orthologs between each tree genome and *Arabidopsis*,

138   Supplementary Table 5). We then manually compiled a list of *Arabidopsis* genes involved in

139   DNA repair from SwissProt/UniProtKB annotations (Supplementary Table 6). We then

140   counted specifically the number of duplicates for genes involved in DNA repair and reported

141   this as the number of orthologs associated with this function (Supplementary Table 3 and 7).

142

143   **<u>Supplementary Discussion</u>**

144   We found that G:C→A:T transitions were the most frequent class of SNVs observed in the

145   Napoleon Oak (Supplementary Figure 7). Ultraviolet (UV) light causes G:C→A:T transitions

146   at dipyrimidine sites in plants[40]. Among the 11 G:C→A:T transitions that we observed, seven

147   were in a dipyrimidine context (Supplementary Table 2). In addition, spontaneous

148   deamination of methylated cytosine leads to thymine change at CpG or CpNG sites [22].

149   However, there were only three G:C→A:T transitions in such a context (Supplementary

150   Table 2). It thus seems plausible that UV light may have caused most of the G:C→A:T

151   transitions we observed, although other factors, such as cytosine deamination and replication

152   errors, may account for other SNVs. Although the oak lineages sampled have not been

153   separated by any meiosis events, which in yeast was found to elevate the generational

154   mutation rate[41], they have been exposed to the natural environment, which in *Arabidopsis* is

155 known to significantly enhance mutation rate when compared to a controlled lab

156 environment[42].

157   Our results throw new light on explanations proposed for differences in the

158 distribution of mating systems between short- and long-lived plants. While many annuals and

159 short-lived plants have undergone evolutionary transitions from outcrossing to selfing[43], often

160 involving a loss of self-incompatibility systems[44], long-lived woody species are more likely

161 to be fully outcrossing[45], including oaks[46]. Theoretical analysis indicates that a high somatic

162 mutation rate could account for this difference, because somatic mutations would contribute

163 to the genetic load of the population and thus to inbreeding depression, disfavouring self-

164 fertilization[1]. Inbreeding depression is indeed higher in long-lived woody species than

165 annuals[47], and the observation of higher inbreeding depression caused by within-branch than

166 between-branch selfing points to the accumulation of different deleterious somatic mutations

167 in different sectors of the plant[3]. However, our finding now challenges the notion that the

168 breeding system of long-lived trees is constrained by a high rate of somatic mutations.

169   The results of our study, in conjunction with those of Burian et al.[14], have important

170 implications for how we should view one of the most fundamental ways in which plants

171 differ from animals – their absence of a germline. In oak, iterative growth of axillary

172 meristems produces terminal branches that carry stem cells. As in other plants, favourable

173 conditions induce stem cells to produce floral buds and ultimately the gametes of the next

174 generation. These stem cells are functionally analogous to germ cells in metazoans and result

175 from a limited number of divisions that prevent an accumulation of replicative errors.

176

References

178 23. Bolger, A.M., Lohse, M. & Usadel, B. Trimmomatic: A flexible trimmer for Illumina
179   Sequence Data. *Bioinformatics* **30**, 2114-2120 (2014).
180 24. Luo, R. *et al.* SOAPdenovo2: an empirically improved memory-efficient short-read de
181   novo assembler. *GigaScience* **1**, 18 (2012).
182 25. Boetzer, M., Henkel, C.V., Jansen, H.J., Butler, D. & Pirovano, W. S. Scaffolding pre-
183   assembled contigs using SSPACE. *Bioinformatics* **27**, 578–579 (2011).

184   26.   Boetzer, M. & Pirovano, W. Toward almost closed genomes with GapFiller. *Genome*
185   *Biol.* **13**, R56 (2012).
186   27.   Segata, N. *et al.* Metagenomic microbial community profiling using unique clade-
187   specific marker genes. *Nature Methods* **9**, 811-814 (2012).
188   28.   English, A.C. *et al.* Mind the gap: Upgrading genomes with Pacific Biosciences RS
189   Long-Read Sequencing Technology. *PLoS One* **7**, 11 (2012).
190   29.   Stanke, M., Steinkamp, R., Waack, S. & Morgenstern, B. AUGUSTUS: a web server
191   for gene finding in eukaryotes. *Nucl. Acids Res.* **32**, W309-312 (2004).
192   30.   Tran, V.D. *et al.* RNA sequencing-based genome reannotation of the dermatophyte
193   *Arthroderma benhamiae* and characterization of its secretome and whole gene
194   expression profile during infection. *mSystems* **1**, e00036-16 (2016).
195   31.   Slater, G.S.C. & Birney, E. Automated generation of heuristics for biological sequence
196   comparison. *BMC Bioinformatics* **6**, 31 (2005).
197   32.   Gardner, P.P. *et al.* Rfam: updates to the RNA families database. *Nucl. Acids Res.* **37**,
198   D136-140 (2009).
199   33.   Sonnhammer, E.L.L., Eddy, S.R. & Durbin, R. Pfam: a comprehensive database of
200   protein families based on seed alignments. *Proteins* **28**, 405-420 (1997).
201   34.   Howald, C. *et al.* Combining RT-PCR-seq to catalog all genic elements encoded in the
202   human genome. *Genome Res.* **22**, 1698-1710 (2012).
203   35.   Keightley, P.D., Ness, R.B., Halligan, D.L. & Haddrill, P.R. Estimation of the
204   spontaneous mutation rate per nucleotide site in a *Drosophila melanogaster* full-sib
205   family. *Genetics* **196**, 313-320 (2014).
206   36.   Lynch, M. & Conery, J.S. The evolutionary fate and consequences of duplicated genes.
207   *Science* **290**, 1151–1155 (2000).
208   37.   Vanneste, K., Van de Peer, Y. & Maere, S. Inference of genome duplications from age
209   distributions revisited. *Mol. Biol. Evol.* **30**, 177-190 (2013).
210   38.   Panchy, N., Lehti-Shiu, M. & Shiu, S.-H. Evolution of gene duplication in plants. *Plant*
211   *Physiol.* **171**, 2294-2316 (2016).
212   39.   Altenhoff, A.M. *et al.* The OMA orthology database in 2015: function predictions,
213   better plant support, synteny view and other improvements. *Nucl. Acids Res.* **43**, D240-
214   D249 (2015).
215   40.   Britt, A.B. DNA damage and repair in plants. *Annu. Rev. Plant Physiol. Plant Mol.*
216   *Biol.* **47**, 75–100 (1996).
217   41.   Rattray, A., Santoyo, G., Shafer, B. & Strathern, J. N. Elevated mutation rate during
218   meiosis in *Saccharomyces cerevisiae*. *PLoS Genet.* **11**, e1004910 (2015).
219   42.   Rutter, M.T., Shaw, F.H. & Fenster, C.B. Spontaneous mutation parameters for
220   *Arabidopsis thaliana* measured in the wild. *Evolution* **64**, 1825-1835 (2010).
221   43.   Stebbins, G.L. Variation and evolution in plants. *Columbia University Press ed.*,
222   (1950).
223   44.   Goldberg, E.E. *et al.* Species selection maintains self-incompatibility. *Science* **330**,
224   493-495 (2010).
225   45.   Barrett, S.C.H., Harder, L.D. & Worley, A.C. The comparative biology of pollination
226   and mating in flowering plants. *Phil. Tran. Royal Soc. London B: Biol. Sci.* **351**, 1271-
227   1280 (1996).
228   46.   Streiff, R. *et al.* Pollen dispersal inferred from paternity analysis in a mixed oak stand
229   of *Quercus robur* L. and *Q. petraea* (Matt.) Liebl. *Mol. Ecol.* **8**, 831-841 (2009).
230   47.   Goodwillie, C., Kalisz, S. & Eckert, C.E. The evolutionary enigma of mixed mating
231   systems in plants: occurrence, theoretical explanations, and empirical evidence. *Annu.*
232   *Rev. Ecol. Evo. Syst.* **36**, 47-79 (2005).
233

234